Dynamics of spiral pairs induced by unidirectional propagating pulses

A. Rabinovitch,[1] M. Gutman,[1] Y. Biton,[1] I. Aviram,[2] and D. S. Rosenbaum[3]
[1]*Department of Physics, Ben-Gurion University of the Negev, Beer-Sheva, 84105, Israel*
[2]*35, Shederot Yeelim, Beer-Sheva, 84730, Israel*
[3]*Heart & Vascular Research Center, Case Western Reserve University, Metrohlth Campus, 2500 Metrohlth Drive, Hamman 322, Cleveland, Ohio 44109, USA*
(Received 27 June 2006; revised manuscript received 5 September 2006; published 12 December 2006)

The dynamics of unidirectionally propagating pulses in a two-dimensional uniform excitable reaction-diffusion medium is investigated. It is shown that under weak diffusion coupling between medium points such a pulse can evolve into a pair of counter-rotating spirals (spiral pair). We analyze the drift of such a pair and examine the collisions between several drifting pairs. It is demonstrated that collisions can result in a special type of reflection or, alternatively, in new types of complex stationary spiral structures. A possible application of these findings for the diagnosis of cardiac arrhythmias is suggested.

DOI: 10.1103/PhysRevE.74.061904 PACS number(s): 87.19.Hh, 87.10.+e, 89.75.Kd

I. INTRODUCTION

Cardiac arrhythmia refers to any abnormal cardiac rhythm which is generally induced either by an abnormal pulse formation or abnormal pulse propagation in altered cardiac tissue [1,2]. During *reentry* for example, a pulse of action potential is spontaneously excited and moves around a ring of tissue in the heart. Such a rotating pulse motion can generate a self-sustained, high-frequency source of reentrant spiral waves that destroy the natural rhythmic cardiac function. The generation of different reentrant waves, as well as their complex dynamics, have obviously attracted an abundant theoretical and applied interest.

Computer models and experiments [3–5] have shown that a reentry process can be generated by applying an initial excitation in a region that is in a relative refractory state, leading to a *unidirectional* propagating pulse (UDP). This is due to an asymmetric spatial change from an absolute refractory to a rest state which creates a one-way conduction block. Recently, it has also been demonstrated [6–8] that by a judicious choice of the shape of the input current triggering pulse, unidirectional propagation of pulses in a uniform excitable medium is feasible and can be obtained both in one- and two-dimensional media.

Such an input current was composed of two adjacent parts with different properties: one component could produce by itself a pair of normally propagating pulses, whereas the second part alone was able to initiate a pair of *decrementally* propagating pulses [9] which completely disappear in the course of time. Simultaneous application of these two components results in a UDP in the following manner: in the 1D system, one of the normal pulses is annihilated after collision with the counterpropagating decremental pulse, while the second decremental pulse eventually disappears, leaving only the second normal pulse. UDPs were numerically obtained in a one-dimensional (1D), ring-shaped periodic strip, as well as in 2D media [8]. In the latter case a UDP was obtained that could preserve its wave form in the course of time or could alternatively shrink and disappear altogether, or spread out and transform into a single concentric wave.

New, interesting features of these UDPs are discussed in the present paper. We show that the UDP can evolve into counter-rotating spirals (hereafter referred to as *spiral pairs*). This feature has been achieved by sufficiently decreasing the diffusion coupling between the points of the excitable medium, a condition which is probably similar to the initiation of spiral waves in susceptible patients whose interconnection between cells has decreased [10]. Such an event can constitute the mechanism of spiral generation in uniform tissue.

The generation, dynamics, and different interactions of spiral pairs were discussed in a number of works [11–16]. In particular, it was shown that a spiral pair can be initiated in an excitable medium by inducing a one-way conduction block. Such a spiral pair was generated by a superthreshold local excitation, properly applied at the "relaxation tail" of a traveling pulse [12]. Various pairwise reactions of different spiral structures, such as a single spiral, a spiral pair, and multiarmed spirals, were also investigated [15]. It was demonstrated that higher-frequency structures can attract, repel, or break up structures of lower frequencies. Here we show that identical drifting spiral pairs can display after collision a particular type of reflection, or alternatively, they can create new types of complex stationary spiral structures. A possible application of our findings for the diagnosis of specific arrhythmias is also discussed.

II. RESULTS

A. UDP-induced spiral pairs

In our two-dimensional (2D) simulations we consider the following FHN system [17]:

$$dv/dt = D\Delta v + f(v,w) + I(t,\boldsymbol{r}),$$

$$dw/dt = g(v,w), \tag{1}$$

where all the variables are in dimensionless units. Here, v is the potential (an excitatory variable) and w is the refractivity (an inhibitory variable). The functions $f(v,w)$ and $g(v,w)$ are given by

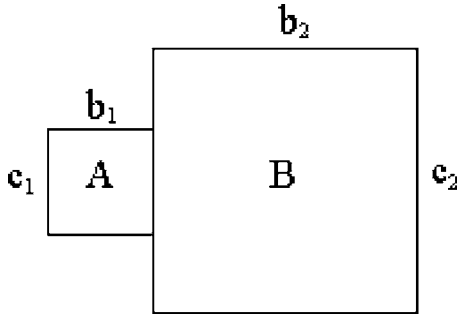

FIG. 1. Spatial contour of the asymmetric input current resulting in the generation of a spiral pair (see text).

$$f = v(v-a)(1-v) - w, \quad g = \varepsilon(v - dw), \tag{2}$$

and $I(t,\boldsymbol{r})$ is the input current. The constants D, a, and ε are, respectively, the diffusion constant, the excitability parameter, and the ratio between the fast and the slow time constants. The constant d depends on the application of the model. We use $D=0.2$, $a=0.12$ (excitable medium), $\varepsilon=0.005$, and $d=3$ throughout, and vary the parameters of the input current $I(t,\boldsymbol{r})$, which is given by

$$I(t,\boldsymbol{r}) = I_1(t)I_2(\boldsymbol{r}), \tag{3}$$

where $I_1(t)$ is a function of time of brief duration, and $I_2(\boldsymbol{r})$ specifies both the spatial location and the amplitudes of the input current. A symmetric form of $I_2(\boldsymbol{r})$ (say, a Gaussian or a square) evidently induces a symmetric response which appears as a circularly propagating wave in 2D. We consider here, on the other hand, an asymmetric I_2. For the 2D case we use the spatial form shown in Fig. 1.

Here c_1, b_1 and c_2, b_2 specify the spatial dimensions of the first (A) and second (B) parts of the input current, respectively. The amplitudes are h_1 (above threshold) and h_2 (below threshold) in A and B, respectively. We use $h_1=0.2$ and $h_2=0.155$ throughout (with the exception of Fig. 3). For a range of values of the control parameters (c_1,b_1,c_2,b_2) such an initial excitation evolves into spiral pairs. Typical values are specified in the figure captions. Note that besides possible important applications (Sec. III), the proposed initial excitation method also yields important features of the spiral pairs. In particular, the structure can drift, thus changing the direction of the generated concentric waves, a change of wave frequency being also possible (see below). The Eqs. (1) were integrated in a rectangular domain with Neumann boundary condition using an Euler integrator. We have run a number of tests in order to assess the range of stability of the algorithm and chose the most convenient values of Δx, Δy, Δt. The size of the integration domain ensures that the morphology of the wave motion is not affected by the boundaries.

To show the creation process of a spiral pair generator, let us consider the time evolution of the system presented in Fig. 2. An asymmetric initial current in Fig. 2(a) generates a unidirectional propagating arclike pulse [Fig. 2(b)], whose free ends begin to curve in opposite directions around two distinct centers, i.e., they transform into tips of two counterrotating spirals [Fig. 2(c)]. The rotation of these spiral tips

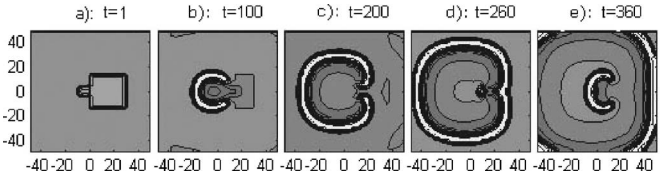

FIG. 2. Time evolution of the UDP-induced spiral pair. $c_1=6$, $b_1=8$, $c_2=26$, $b_2=28$, $\Delta t=0.1$, $\Delta x=\Delta y=2$.

continues until the arms of the two spirals collide and partially annihilate [Fig. 2(d)]. As a result, two structures appear simultaneously: an outward-moving concentric pulse and an inward-moving arclike pulse [Fig. 2(e)]. The arclike pulse, being similar to the one of Fig. 2(b), causes a repetition of the entire process, resulting in the appearance of two new oppositely moving structures, one concentric and the other arclike, and so on. Note that under the *strong diffusion* conditions in [8], the free ends of both arms completely annihilated each other, leading to a *single* outward-propagating pulse.

In order to assess the range of parameters for which the UDP-induced spiral pairs can be generated, we kept parameters ε, d, c_1, b_1, c_2, b_2, and h_1 fixed, and varied the parameters D, a, and h_2. The parameters $\varepsilon=0.005$ and $d=3$ are the same as in Ref. [18], where these values are associated with normal cardiac function. In the present study, heart dysfunctions are associated with variations of D (conductivity) and a (excitability), whose important role to the generation of pathological spiral waves has been discussed (e.g., [2,3,12]). Figure 3 provides the range in the a-D plane where such spiral pairs are obtained. The rather extended a range coincides with the boundaries of the excitable region. For larger a values no pulses propagate in the medium whatsoever. The amplitude h_2 was selected in each case so that decrementally propagating pulses could be generated. This basic condition determines the lower and upper D boundaries in Fig. 3. It turns out that the appropriate h_2 value can be empirically derived from the following equation:

$$h_2 = 0.049 + 0.9a. \tag{4}$$

Below the lower boundary of the SP domain, h_2 cannot generate any propagating pulses, whereas above the upper

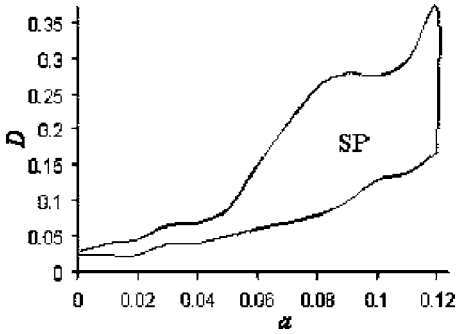

FIG. 3. The (a,D) plane showing the range of values where UDP-induced spiral pairs (SP) can be generated. $\Delta t=0.5$, $\Delta x=\Delta y=2$, $c_1=10$, $b_1=10$, $c_2=30$, $b_2=50$, $h_1=0.2$

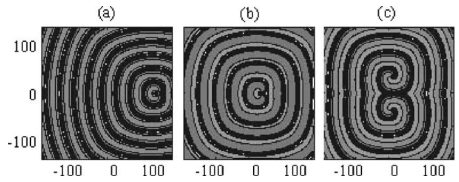

FIG. 4. Drifting (a, b) and stationary (c) spiral pairs. All spiral pairs were initiated at the same location. The spiral pair with the smallest distance between its centers [Fig. 4(a)] displays the fastest drift. $t=20\,000$, $\Delta t=0.5$, $\Delta x=\Delta y=2$. (a): $c_1=10$, $b_1=8$, $c_2=22$, $b_2=48$; (b): $c_1=8$, $b_1=8$, $c_2=22$, $b_2=48$; (c): $c_1=118$, $b_1=8$, $c_2=118$, $b_2=58$.

boundary, h_2 generates normally propagating pulses. We have also checked the robustness of our calculations by adding white noise to the function f of Eq. (2). For noise amplitude below 10% of the threshold current, spiral pairs are feasible; otherwise, only a single target wave is obtained.

B. Properties

The obtained spiral pair thus represents a localized source of concentric waves which can slowly drift along the symmetry axis. Although such a drift has been discussed in several works (see, e.g., [16,19] and references therein), its underlying mechanism, to our knowledge, is still poorly understood. We assert that this phenomenon can be explained by the fact that every new arclike pulse is created from an *outward-moving* wave [see, e.g., Figs. 2(c) and 2(d), which leads to a change of location of the subsequent spiral pairs along the x direction in Fig. 2]. This assumption is further confirmed by the following arguments. Since the arm of each spiral of the pair simultaneously rotates around its spiral center and propagates away from this center in the positive x direction, the resulting velocity of the contact point between counter-rotating arms should decrease with increasing distance between the centers of the spiral pair. This velocity determines the initial site of the ensuing arclike source after collision, and therefore the drift velocity should decrease as well [see Figs. 4(a) and 4(b)]. Finally, if the distance between the centers of counter-rotating spirals is above a specific value, the arclike source emerges at the same location as the previous one, and the system becomes stationary [Fig. 4(c)]. Note also that during a head-on collision between two identical spiral pairs, the point where the arclike pulses are generated becomes fixed and the spiral structures become stationary, as described in Sec. II C.

Another important feature of a spiral pair is the frequency of the generated outgoing concentric waves. The frequency is measured as the reciprocal value of the time interval between waves passing through a point of the medium at a relatively distant location from the spiral pair center. It was previously reported [15] that such a frequency is typically higher than that obtained for a single spiral. Our simulations show that this frequency, as well as the type of corresponding oscillations, depends on the distance between the centers of the two counter-rotating spirals and can also change in the course of time (Fig. 5). Note that the time step Δt used in the numerical integration can also affect the

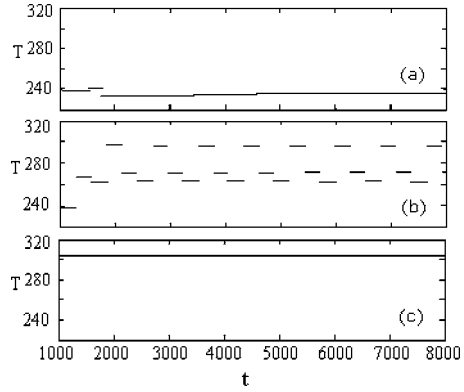

FIG. 5. Time evolution of the period T of local oscillations induced by drifting (a), (b) and stationary (c) spiral pairs shown in Fig. 4.

described characteristics of the spiral pairs (see also [19]). Most interestingly, the type of oscillations of spiral pairs can determine the character of their interactions. In particular, during the collision of identical spiral pairs, either in a transient aperiodic or a multiperiodic regime, there arise stable spiral structures (Sec. II C), whereas the collision of two identical spiral pairs in a single periodic regime results in a special type of reflection (see Sec. II D).

C. Stationary spiral structures

The simulation shows that head-on collisions of two identical drifting spiral pairs can generate a new type of stationary spiral structures. The underlying mechanism of such structures is similar to that of the creation of a single spiral pair. Here again, collision and partial annihilation of free ends of two counter-rotating spirals leads to the creation of a small moving arc which evolves into a new spiral pair. But here, the upper and lower spirals belonging to *different* spiral pairs collide and create two small arcs approaching each other along the y axis [Figs. 6(a)–6(d)]. Their collision [Fig. 6(e)] in turn creates two new small arcs moving apart along the x axis [Figs. 6(f) and 6(g)]. Later on, these small arcs evolve into two new approaching spiral pairs, whose head-on collision completes a full dynamical cycle of this stationary spiral structure [Fig. 6(h)].

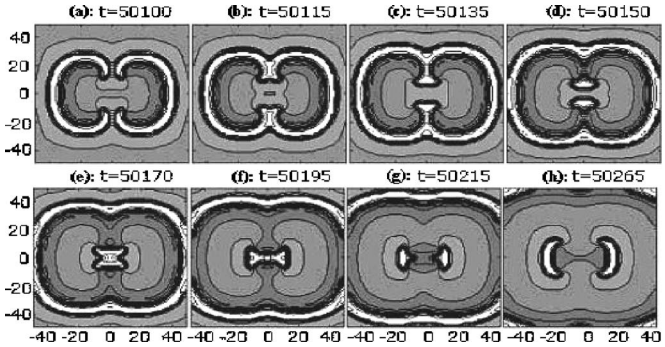

FIG. 6. Dynamics of the stationary beating spiral structure produced by a head-on collision of two drifting spiral pairs analogous to the pair shown in Fig. 4(b).

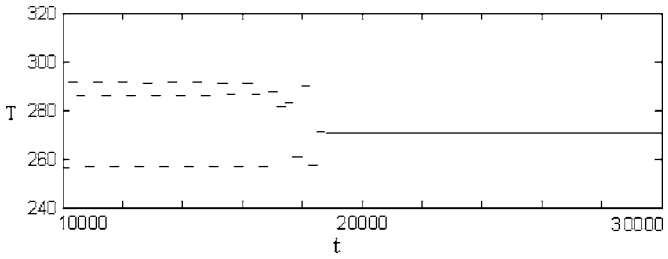

FIG. 7. Evolution of oscillations measured at the point $(x=1, y=100)$ "far away" from the site of collision of two spiral pairs. In the course of time, period-3 oscillations are substituted by period-1 oscillations with $T=267$.

It is interesting to note the stabilizing effect accompanying the generation of this structure. Period-3 oscillations measured at the point (1,100), far from the approaching spiral pairs, are modified by collision and reduce finally to a period-1 beating of the stationary oscillating spiral structure (Fig. 7).

A stationary spiral structure of another type can be generated by the collision of four spiral pairs approaching each other along the x and y axes. In this case, four small arcs are simultaneously created and approach each other across two perpendicular lines located at 45° to the principal axes. The four arcs collision produces an unstable cross-shaped formation, which breaks up into four new small arcs moving apart along the x and y axes. These small arcs in turn evolve into four spiral pairs which approach each other, thus completing a full cycle of this stationary spiral structure [Figs. 8(a)–8(d)]. Here again, a similar stabilizing effect is observed which results in simplified period-1 oscillations similar to the situation shown in Fig. 7, but now with a somewhat higher oscillation frequency ($T=260$).

D. Reflection

If two spiral pairs (Fig. 9) collide under some specified initial conditions, different from those of Fig. 6, the pairs are "reflected" in opposite directions along the y axis. This type of interaction was observed, for example, with the initial geometry of the triggering pulse specified in Fig. 4(b), and also in Fig. 9. As in Fig. 6, here again, two small arclike pulses become detached from the *moving* sections of the spiral pairs [Figs. 9(d)–9(g)]. However, the wider spreading of spirals causes the next contact to take place at a point situated farther away along the y axis. The final y direction motion of the initially approaching spiral pairs may thus be

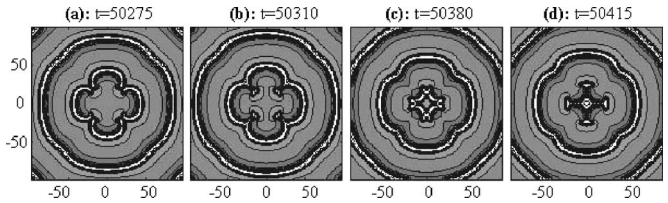

FIG. 8. Dynamics of the stationary spiral structure produced by the collision of four drifting spiral pairs. The parameters are the same as in Fig. 4(b).

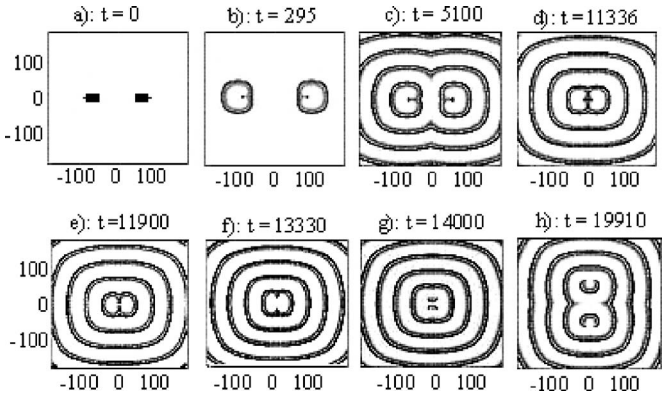

FIG. 9. Head-on collision of two spiral pairs resulting in their reflection along the bisector (y axis). $\Delta t=0.5$, $\Delta x=\Delta y=2$, $c_1=10$, $b_1=10$, $c_2=30$, $b_2=50$.

regarded as a new kind of reflection [Fig. 9(h)]. The characteristic feature of such a reflection is that after collision, the spiral pairs propagate along a bisector to the angle between the directions of their initial motion. For a head-on collision along the x axis, the bisector coincides with the y axis.

We have also examined the collision of two pairs moving at 45° and 135° with respect to the x axis (the angle of incidence being 90°), as shown in Fig. 10(a). After collision the spiral pairs drift apart along the x axis. Figure 10 demonstrates the process of reflection into the bisector directions.

As mentioned in Sec. II B, such reflection is observed only under collision of spiral pairs which display simple periodic oscillations. Comprehensive analysis of these results is a subject matter of future investigations.

III. DISCUSSION

Let us now consider the UDP-induced spiral pairs, both for a better understanding of some reentry cardiac arrhythmias and as a potential diagnostic method.

A. Mechanism of figure-eight reentry

A frequently observed pattern in reentry-type heart failures, such as ventricular tachycardia (VT) and/or

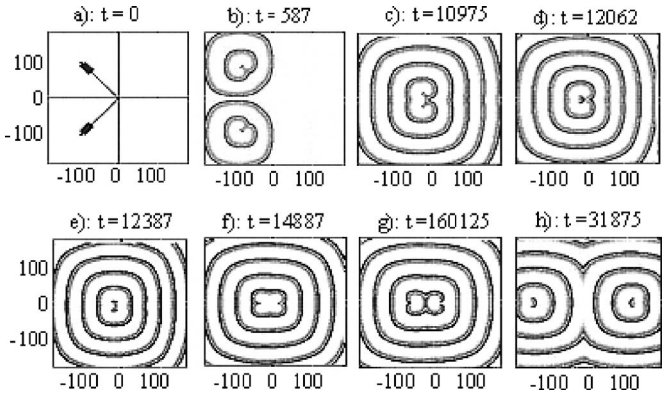

FIG. 10. Collision of two pairs oriented at 45° and 135° with respect to the x axis. $\Delta t=0.5$, $\Delta x=\Delta y=2$, $c_1=20$, $b_1=24$, $c_2=30$, $b_2=70$.

ventricular fibrillation (VF), is the so-called figure-eight reentry [20–22], which is composed of two counterrotating spiral waves. The generation of such spiral pairs and their features were often associated with the existence of different heterogeneities within the excitable cardiac tissue [23–26]. Based on the present work, an additional mechanism for such a figure-eight reentry generation appears to be possible, in which the dominant role is played by spatially asymmetric pathological excitations similar to those presented here.

Note also that the stationary spiral structures of Fig. 6 are similar to the quatrefoil reentry pattern, previously obtained only in a more complicated spatially anisotropic bidomain model [12,27].

B. Modified electrophysiological testing

The method of creating a pair of spirals may be used to facilitate the induction of reentrant arrhythmias. Specifically, it may improve the yield of inducing ventricular tachycardia by programmed cardiac stimulation during electrophysiology (EP) testing. EP testing is a diagnostic test for patients with a suspected arrhythmia [28,29]. Using a catheterization procedure directly into the heart, its electrical performance is recorded both under normal and catheter stimulations. One piece of information obtained in this testing is whether VT/VF can be triggered by this stimulation. At the present time, only a positive EP study carries prognostic significance, while a negative study has been associated with significant even rates (relative risk 1.4 in MADIT I). We hypothesize that the poor sensitivity of EP testing arises in part from the difficulty or even complete inability to induce a unidirectional block for VT induction. The unidirectional stimulation (pacing) described in our previous papers [6–8] could thus be used to induce figure-eight reentry-type arrhythmias for the purpose of risk stratification. Especially, VT induction should be easier to achieve with unidirectional as compared to conventional pacing, which can only induce VT with aggressive pacing protocols.

[1] J. Keener and J. Sneyd, *Mathematical Physiology* (Springer, New York, 1998).
[2] A. V. Panfilov and A. V. Holden, *Computational Biology of the Heart* (Wiley, New York, 1997).
[3] C. F. Starmer *et al.*, Biophys. J. **65**, 1775 (1993).
[4] I. N. Motoike, K. Yoshikawa, Y. Iguchi, and S. Nakata, Phys. Rev. E **63**, 036220 (2001).
[5] I. Sendina-Nadal, M. de Castro, F. Sagues, and M. G. Gesteira, Phys. Rev. E **66**, 016215 (2002).
[6] A. Rabinovitch, I. E. Ovsyshcher, I. Fleidervish, and E. Crystal, U.S. Patent No. 6,463,330 B1 (8 October 2002).
[7] E. Crystal, I. Fleidervish, A. Rabinovitch, and I. E. Ovsyshcher, in *Cardiac Arrhythmias and Device Therapy: Results and Perspectives for the New Century*, edited by I. E. Ovsyshcher (Futura Publishing Company, Inc., Armonk, NY, 2000) pp. 41–46.
[8] M. Friedman, I. E. Ovsyshcher, I. Fleidervish, E. Crystal, and A. Rabinovitch, Phys. Rev. E **70**, 041903 (2004).
[9] Y. Horikawa, Phys. Rev. E **50**, 1708 (1994); Biol. Cybern. **79**, 251 (1998).
[10] A. Pumir *et al.*, Biophys. J. **89**, 2332 (2005).
[11] E. A. Ermakova, A. M. Pertsov, and E. E. Shnol, Physica D **40**, 185 (1989).
[12] A. T. Winfree, *When Time Breaks Down: The Three Dimensional Dynamics of Electrochemical Waves and Cardiac Arrhythmias* (Princeton University Press, Princeton, NJ, 1987).
[13] I. Schebesch and H. Engel, Phys. Rev. E **60**, 6429 (1999).
[14] I. S. Aranson and L. M. Pismen, Phys. Rev. Lett. **84**, 634 (2000).
[15] R. M. Zaritski and A. M. Pertsov, Phys. Rev. E **66**, 066120 (2002).
[16] C. Zemlin, K. Mukund, M. Wellner, R. Zaritsky, and A. Pertsov, Phys. Rev. Lett. **95**, 098302 (2005).
[17] R. FitzHugh, Biophys. J. **1**, 445 (1961).
[18] A. Rabinovitch, I. Aviram, N. Gulko, and I. E. Ovsyshcher, J. Theor. Biol. **196**, 141 (1999).
[19] M. Ruiz-Villarreal, M. Gómez-Gesteira, and V. Pérez-Villar, Phys. Rev. Lett. **78**, 779 (1997).
[20] G. R. Ivanitskii, V. I. Krinskii, A. V. Panfilov, and M. A. Tsyganov, Biophysics (Engl. Transl.) **34**, 319 (1989).
[21] P. Chen, A. Garfinkel, J. N. Weiss, and H. S. Karagueuzian, Chaos **8**, 127 (1998).
[22] D. L. Beaudoin and B. J. Roth, PACE **29**, 496 (2006).
[23] W. Quan and Y. Rudy, Circ. Res. **66**, 367 (1990).
[24] A. V. Panfilov and B. N. Vasiev, Physica D **49**, 107 (1991).
[25] I. Banville *et al.*, Circ. Res. **85**, 742 (1999).
[26] K. H. W. J. Ten Tusscher and A. V. Panfilov, Am. J. Physiol. Heart Circ. Physiol. **284**, H542 (2003).
[27] B. J. Roth, J. Theor. Biol. **230**, 445 (2004).
[28] E. R. Behr, P. Elliott, and W. J. McKenna, Card. Electrophysiol. Rev. **6**, 482 (2002).
[29] D. M. Bosen and M. A. Flemming, Dimens Crit. Care Nurs. **22**, 10 (2003).